NATIONAL ADVISORY COMMITTEE FOR AERONAUTICS

WARTIME REPORT

ORIGINALLY ISSUED
February 1945 as
Advance Restricted Report L5A13

THE INFLUENCE OF VERTICAL-TAIL DESIGN AND DIRECTION

OF PROPELLER ROTATION ON TRIM CHARACTERISTICS

OF A TWIN-ENGINE-AIRPLANE MODEL WITH ONE

ENGINE INOPERATIVE

By Marvin Pitkin, John W. Draper, and Charles V. Bennett

Langley Memorial Aeronautical Laboratory
Langley Field, Va.

NACA

WASHINGTON

NATIONAL ADVISORY COMMITTEE FOR AERONAUTICS

ADVANCE RESTRICTED REPORT

THE INFLUENCE OF VERTICAL-TAIL DESIGN AND DIRECTION

OF PROPELLER ROTATION ON TRIM CHARACTERISTICS

OF A TWIN-ENGINE-AIRPLANE MODEL WITH ONE

ENGINE INOPERATIVE

By Marvin Pitkin, John W. Draper, and Charles V. Bennett

SUMMARY

Tests have been made in the Langley free-flight tunnel to determine the influence of mode of propeller rotation and vertical-tail design upon the trim characteristics of a model of a twin-engine airplane with one engine inoperative. The test model was mounted on a trim stand, which allowed freedom in roll and yaw under conditions simulating those required by the NACA and the Army Air Forces for asymmetric-power operation in flight. The seven vertical-tail designs tested included three tails of low aspect ratio and of different area, one twin tail of low aspect ratio, two tails of high aspect ratio and with different rudder areas, and one all-movable tail of high aspect ratio equipped with a linked tab. All tests were made with the flaps down.

The tests showed that the effect of mode of propeller rotation upon the directional trim characteristics of the model operating with asymmetric power was considerable. Propeller rotation in which the upper tips rotate outboard toward the wing tip (outboard rotation) generally created more severe out-of-trim conditions than inboard rotation.

The all-movable tail design was found to be more effective than the other designs tested in nullifying the effects of asymmetric power. The conventional tail designs with high aspect ratio were more effective than the designs with low aspect ratio in this respect. The single vertical tails were generally more effective in trimming the yawing moments created by asymmetric power than twin vertical tails of the same aspect ratio and equal

area, particularly when the rudder was free. At small
angles of sideslip, however, the moments caused by
asymmetric power were more readily trimmed by deflecting
the rudders of the twin tails than by deflecting the
rudder of a single tail.

The trimming effectiveness of the vertical tail in-
creased almost directly with vertical-tail area but in-
creased at a decreasing rate with rudder deflection and
chord.

When the rudder was free, the addition of dorsal-
and ventral-fin areas permitted increases in the asym-
metric power balanced by the tail surface at moderate
angles of sideslip.

INTRODUCTION

The failure of one or more engines of multiengine
airplanes introduces a sudden and severe demand upon the
directional stability and control of those airplanes.
Such failures result in the instantaneous application of
large yawing moments that must be neutralized either by
the rudder control or by the directional stability of the
airplane. In addition, asymmetric power conditions create
rolling moments that must be balanced by aileron deflection
in order to maintain straight flight. This aileron de-
flection creates additional yawing moments that require
further trimming by the vertical tail surfaces. For multi-
engine airplanes, then, the asymmetric power condition
generally imposes the most severe requirements for di-
rectional stability and control and to a large extent
dictates the design of the vertical tail surfaces of these
airplanes.

An investigation has therefore been carried out in
the Langley free-flight tunnel to provide data concerning
the relative merits of seven vertical-tail designs and
two modes of propeller rotation under conditions of asym-
metric power. The NACA and Army flying-qualities require-
ments (references 1 and 2) for directional stability and
control of airplanes operating with asymmetric power were
used to establish the test conditions. The results of the
investigation are reported herein.

A $\frac{1}{20}$-scale model of a conventional twin-engine airplane in the medium-bomber class (the North American B-28 airplane) was used in the tests. The model was mounted on a test stand, which allowed freedom in yaw and roll. The effects of asymmetric power could thus be visually observed from changes in the model attitude.

The seven vertical-tail designs studied in this investigation varied in either aspect ratio, total tail area, rudder area, or general arrangement. Tests were made with rudders fixed and free, and the effects of adding various dorsal and ventral fins were studied with the rudders free. The effect of mode of rotation of the operating propeller upon the vertical-tail characteristics was investigated for all tail arrangements. All tests were made with the flaps down.

SYMBOLS

C_L lift coefficient $\left(\dfrac{\text{Lift}}{q S_w}\right)$

C_l rolling-moment coefficient $\left(\dfrac{\text{Rolling moment}}{q S_w b_w}\right)$

C_n yawing-moment coefficient $\left(\dfrac{\text{Yawing moment}}{q S_w b_w}\right)$

C_{n_β} rate of change of yawing-moment coefficient

with angle of sideslip $\left(\dfrac{\partial C_n}{\partial \beta}\right)$

T_c thrust coefficient for one engine $\left(\dfrac{T_e}{\rho V^2 D^2}\right)$

D propeller diameter, feet

ρ density of air, slug per cubic foot

V free-stream airspeed, feet per second

$V_{\text{take-off}}$ velocity at end of take-off run, feet per second

$V_{\min}$ stalling speed with flaps down, feet per second

q free-stream dynamic pressure, pounds per square foot $\left(\dfrac{1}{2}\rho V^2\right)$

T_e effective thrust of one engine, pounds

η propeller efficiency, percent

W gross weight, pounds

S_w wing area, square feet

bhp   brake horsepower of full-scale airplane simulated by model

thp   thrust horsepower

δ_a combined aileron deflection, degrees

δ_r rudder deflection, positive when trailing edge is to left, degrees

δ_f flap deflection, positive when trailing edge is down, degrees

δ_e elevator deflection, degrees

δ_T tab deflection of all-movable tail, positive when trailing edge is to left, degrees

i_t tail incidence of all-movable tail with respect to center line of fuselage, degrees

α angle of attack, degrees

α_t local angle of attack of vertical tail, degrees

β angle of sideslip, degrees

A aspect ratio of vertical tail $\left(b_t^2 / S_t\right)$

S_t area of vertical tail, square feet

S_b balance area of rudder, percent rudder area

S_r rudder area, square feet

b_t span of vertical tail, feet

b_w wing span, feet

APPARATUS

Wind Tunnel

The tests were made in the Langley free-flight tunnel, a complete description of which will be found in reference 3. The tunnel was locked at an angle of pitch of $0°$ for all tests.

Trim Stand

All tests were made on a trim stand, which was securely fastened to the floor of the wind tunnel. This stand was so constructed as to allow the model freedom in roll and yaw about the stability axes of the model. The stability axes are a system of axes in which the Z-axis is in the plane of symmetry of the airplane perpendicular to the relative wind. The X-axis is in the plane of symmetry perpendicular to the Z-axis. The Y-axis is perpendicular to the plane of symmetry. The origin of the stability axes is at the center of gravity of the airplane, which for the present tests was located on the fuselage center line 25 percent of the mean aerodynamic chord behind the leading edge.

Photographs of the model mounted on the trim stand are given as figure 1 and the construction of the stand is illustrated in figure 2. Figure 2 shows that bearing A permits freedom in roll and bearing B permits freedom in yaw. A calibrated coil spring was inserted in bearing A to provide stability in roll. This alteration made possible the measurement of unbalanced rolling moments as a function of the angle of bank and thereby facilitated the trimming of these moments by means of aileron deflection. Both bearings A and B were equipped with ball bearings to keep frictional effects to a minimum.

The trimming fin shown in figure 2 was added to the trim stand to neutralize the drag yawing moments caused when the wind was on by the forward struts at an angle of yaw. Since this fin area was such that the trim stand was in complete equilibrium of yawing moments $\left(C_{n_\beta} = 0\right)$ over the yaw range tested, the trim stand did not affect the directional stability characteristics of the model.

Model

The model used in the investigation was a $\frac{1}{20}$-scale model of the North American B-28 airplane. A three-view drawing and a photograph of the model are given as figures 3 and 4, respectively.

The model was equipped with 2 four-blade propellers having a diameter of 8.50 inches and set at an angle of pitch of 20°. Power was furnished by a direct-current controllable-speed electric motor rated 1/8 horsepower at 15,000 rpm. The left propeller, which was kept inoperative during the tests, was so mounted as to windmill freely. The right propeller, which was used as the operating propeller for all tests, was geared to the motor at a ratio of 1:3. Provision was made for reversal of the direction of propeller rotation. The model was equipped with partial-span slotted flaps (fig. 3), which were deflected 45° for all tests.

Sketches of the vertical-tail designs used in the investigation are shown in figure 5 and sketches of the dorsal- and ventral-fin areas utilized in the rudder-free tests, in figure 6. Tail 2 represents the original vertical tail surface of the full-scale airplane and is considered typical of conventional vertical-tail design. The dimensional characteristics of this tail were varied to form the other vertical-tail designs. All vertical tails were constructed of the NACA 0012 section. In order to maintain similitude of hinge-moment characteristics as far as practicable, all rudders were of identical blunt-nose balance type with a balance area 12.2 percent of the rudder area. This type of rudder is of negative floating tendency and trails with the wind when free.

The dimensional characteristics of the full-scale airplane are given in the following table:

Wing:

        Area, sq ft 675.90
        Span, ft 72.61
        Aspect ratio 7.80
        Root chord, in. 161.13
        Tip chord, in. 67.00
        Mean aerodynamic chord, in. 120.09
        Root section .... NACA 23017

Tip section .... NACA 4409R
Percent chord line with zero sweepback 33
Sweepback at leading edge, deg 4.2
Dihedral angle, deg 2
Incidence, deg 3
Geometric twist (washout), deg 2.5
Taper ratio 2.4:1

Fuselage:

Length, ft 54.5
Section .... Circular
Frontal area, sq ft 38.5

Horizontal tail:

Total area, sq ft 183.20
Span, ft 26.85
Aspect ratio 3.94
Dihedral angle, deg 0
Stabilizer setting, deg 1.50
Length from hinge of elevator to center of
    gravity of airplane, ft 28.90
Elevator balance area, sq ft 10.63
Elevator area behind center line of hinge, sq ft 53.00

Vertical tail 2:

Total area, sq ft 74.90
Span, ft 10.68
Aspect ratio 1.54
Length from hinge line of rudder to center of
    gravity of airplane, ft 27.40
Fin area, sq ft 35.66
Rudder area, sq ft 39.24
Rudder-balance area, sq ft 9.14
Rudder area behind hinge line, sq ft 30.10

(Pertinent data for tails 1, 3, 4, 5, 6, and 7 are given
    in fig. 5.)

Aileron (one of two):

Area behind hinge line, sq ft 20.91
Span, ft 11.41
Mean chord, in. 17.0

Flap:

    Total flap area, sq ft 80.3
    Total span, ft 38.4
    Type .... Slotted

SPECIFICATIONS AND CRITERIONS

The NACA and Army flight requirements for multiengine airplanes operating with asymmetric power were chosen to establish the proper test conditions. No separate attempt was made to reproduce the Navy specifications for asymmetric power because of the close similarity between the Navy and the NACA specifications.

Specifications for Directional Control

(Rudder Fixed)

The NACA and Army specifications (references 1 and 2, respectively) for directional control of airplanes operating with asymmetric power are as follows:

NACA requirement (II-E) 3.- "The rudder control should be sufficiently powerful to provide equilibrium of yawing moments at zero sideslip at all speeds above 110 percent of the minimum take-off speed under the following conditions:

        a. Airplanes with two or three engines:
            With any one engine inoperative
            (propeller in low pitch) and the
            other engine or engines developing
            full rated power."

Army requirement E-2c(1)(c).- "The rudder control shall be powerful enough to trim a multi-engine airplane for straight flight with less than 10 degrees of sideslip at 1.2 V_{s_h} $\left[V_{s_h} \right.$ = stalling speed of the airplane, throttles closed, gear down, flaps in best take-off condition$\left. \right]$ when the throttle on an outboard engine is abruptly closed (propeller in low pitch) and the other engine or engines are developing full take-off power. The flaps shall be in the take-off setting, and the gear shall be down...."

Specifications for Directional Stability

(Rudder Free)

The NACA specification (requirement (II-F) 4 of reference 1) relating to the requirements for directional stability with rudder free under asymmetric power conditions is as follows:

"The yawing moment due to sideslip (rudder free with airplane trimmed for straight flight on symmetric power) should be such that straight flight can be maintained by sideslipping at every speed above 140 percent of the minimum speed with rudder free with extreme asymmetry of power possible by the loss of one engine."

Criterion for Vertical-Tail Effectiveness

under Asymmetric Power Conditions

Each of the specifications previously listed requires the directional control or the directional stability of the airplane in question to be sufficiently powerful to balance the yawing moments created by asymmetric power under certain specified flight conditions. It follows that the vertical-tail effectiveness in flight may be gaged by the maximum amount of asymmetric power which such a tail can balance under the specified conditions. In this investigation, therefore, the maximum asymmetric power permissible under the airspeed and trim conditions specified by the Army and the NACA was used to evaluate the effectiveness of the vertical tails tested.

It should be observed that the flight specifications require that straight flight or complete equilibrium of lateral forces and moments be maintained. In order to maintain such equilibrium in flight, the ailerons must be deflected so that the rolling moments caused by asymmetric power are balanced and the airplane assumes an attitude of bank, which nullifies the side force created by rudder deflection and/or angle of sideslip. Inasmuch as an attitude of bank does not affect the trim requirements of the vertical tail surface, no attempt was made in the tests to simulate the balance of side force by angle of bank. Aileron deflection, however, directly affects directional trim by virtue of the yawing moments created by such deflections. Consequently, the ailerons were so adjusted

for all tests as to maintain complete balance of aero-
dynamic rolling moments and thereby to simulate flight
conditions correctly.

TESTS

Test Conditions

The test lift coefficient was established from con-
sideration of the specified airspeeds in the Army and NACA
requirements. These values were converted to lift-
coefficient forms as follows:

The NACA requirement (II-E) 3 a (rudder fixed) speci-
fies an airspeed equal to 1.10 times the take-off speed.
If $V_{take-off}$ is assumed equal to $1.2V_{min}$, the airspeed
requirement for this specification is equal to $1.32V_{min}$.
If the maximum lift coefficient of the B-28 airplane is
assumed equal to 2.0, the specified lift coefficient cor-
responding to $1.32V_{min}$ is defined by the expression

$$2.0\left(\frac{V_{min}}{1.32V_{min}}\right)^2$$ which equals 1.15. In a similar manner,

the lift coefficient necessary to satisfy NACA requirement
(II-F) 4 (rudder free) was found to be 1.02. The lift
coefficient necessary to satisfy the Army requirement
(rudder fixed) was calculated as 1.39. Because it was as-
sumed that slight changes in lift coefficient would not
affect the model test results if the correct values of
thrust coefficient were used, all tests were run at a con-
stant angle of attack of 5°, which corresponded to a lift
coefficient of 1.10.

All tests were run at a test velocity of 40 feet per
second, which corresponds to a test Reynolds number of
128,000 based on the mean aerodynamic chord of 0.503 foot.
The aileron deflections for all tests were adjusted to
provide equilibrium of rolling moments.

Test Procedures

Rudder fixed.- In the tests with rudder fixed, the
model was mounted on the stand with the rudder deflected
in the direction that counteracted the yaw caused by

asymmetric power. Measurements were then taken of the maximum amount of asymmetric thrust the rudder would balance at angles of yaw of 0° and 10° for rudder deflections of 0°, 5°, 10°, 20°, and 30°.

Rudder free.- The tests with rudder free were made by measuring the amount of asymmetric thrust and angle of yaw produced by asymmetric power for various angles of yaw up to the angle at which directional instability was encountered. Tests with rudder free were made of the model with each of the following vertical-tail arrangements:

(1)   Vertical tail alone

(2)   Vertical tail plus dorsal fin a

(3)   Vertical tail plus dorsal fin b

(4)   Vertical tail plus ventral fin a

(5)   Vertical tail plus ventral fin a
        plus dorsal fin a

The absolute dorsal- and ventral-fin areas required for each test were determined from the percentages of the vertical tails being tested given in figure 6. No tests were made to determine the influence of auxiliary fin area upon the characteristics of twin tail 4.

Power calculations.- The thrust coefficients that were obtained in the tests of the model were converted to the simulated asymmetric brake horsepower of the full-scale airplane by means of the relationship

$$bhp = \frac{thp}{\eta}$$

$$= \frac{T_e V}{550\eta}$$

or

$$bhp = \frac{T_c \left(\dfrac{2\dfrac{W}{S_W}}{C_L}\right)^{3/2} D^2}{550\eta\rho^{1/2}} \qquad (1)$$

The full-scale propeller efficiency η was assumed to be equal to 0.75 for the calculations. Values of wing loading W/S_w and propeller diameter D were obtained from the full-scale characteristics of the North American B-28 airplane and were equal to 47.5 pounds per square foot and 14.7 feet, respectively. The value of the mass density of air ρ was chosen as 0.00238, which is its value at sea level under standard atmospheric conditions. Substitution of these values in equation (1) yields the relationship

$$bhp = \frac{T_c}{C_L^{3/2}} 9900 \qquad (2)$$

The values of C_L in equation (2) are those corresponding to the airspeed specified in the Army and the NACA requirements and were determined as shown in the section entitled "Test Conditions." Substituting these values of lift coefficient in equation (2) yields the expressions defining the conversion of model thrust coefficient T_c to the estimated full-scale brake horsepower, which are: For rudder fixed,

NACA requirement

$$bhp = 8050T_c \qquad (3)$$

Army requirement

$$bhp = 6070T_c \qquad (4)$$

For rudder free,

NACA requirement

$$bhp = 9620T_c \qquad (5)$$

RESULTS AND DISCUSSION

The data obtained in the investigation are plotted in figures 7 to 18. Figure 7 shows the rolling-moment coefficients produced by the ailerons used in the tests. Figures 8 to 10 present the values of the asymmetric-thrust coefficient balanced by means of rudder deflection.

Figures 11 to 13 give the values of the asymmetric-thrust
coefficient balanced by the yawed model with rudder free.
Data showing the influence of dorsal- and ventral-fin areas
upon trim characteristics are presented in figures 14 to 18.

The test data in figures 8 to 13 were rearranged and
converted to values of full-scale brake horsepower in
figures 19 to 24. An index to all figures is presented
as table I.

Effect of Mode of Propeller Rotation

The mode of propeller rotation in which the upper
blade tips move toward the fuselage is henceforth designated
inboard rotation. The rotation in which the upper blade
tips move out toward the wing tip is designated outboard
rotation. Almost all conventional airplanes are equipped
with right-hand propellers. On multiengine airplanes,
the direction of propeller rotation with respect to the
wing tips (inboard or outboard) is therefore determined
by the location of the propeller. If the right engine
fails, the direction of the operating propeller rotation
is inboard and the airplane yaws in a positive sense.
For left-engine failures, the operating propeller rotates
outboard and the airplane yaw is negative. The results
of the present investigation show that use of different
modes of propeller rotation caused considerable difference
in trim characteristics of an airplane operating under
asymmetric power.

With only one exception, the data presented in
figures 8 to 13 indicate that the use of outboard propeller
rotation decreased the values of permissible asymmetric-
thrust coefficient balanced by any given vertical-tail con-
figuration and that this mode of rotation would therefore
determine the minimum vertical-tail size. The exception
occurred when twin tail 4 operated under the Army specifi-
cations (fig. 9); in these tests inboard rotation was less
favorable than outboard rotation.

The difference in asymmetric power balanced by a given
tail arrangement with either of the two modes of rotation
appeared to increase in magnitude with the amount of di-
rectional stability and of control being applied. The
largest differences occurred at large rudder angles and for
tails 5, 6, and 7, which have high aspect ratios. Particu-
larly large effects of propeller rotation were observed when
the rudder was free.

The magnitude of effect of reversing the propeller rotation has been illustrated in figure 19. This figure presents the calculated values of permissible brake horsepower for both modes of propeller rotation for the representative rudder deflection of 20° (figs. 19(a) and 19(b)) and for that angle of sideslip at which directional instability was encountered in the tests with rudder free (fig. 19(c)). This angle of sideslip was between 10° and 12° for almost all the conditions tested. The results presented in figure 19 show that the difference in asymmetric power balanced by the vertical tail for inboard and outboard rotation was about 400 horsepower for most conditions and was as large as 1000 horsepower for some.

The effects of changing the direction of propeller rotation appear to be explained by the data of reference 4. Reference 4 concludes that use of inboard propeller rotation with the flaps down caused the slipstream to converge toward the tail and thereby increased the contribution of the tail surfaces to directional stability for small to moderately large angles of yaw. This slipstream displacement would result in a beneficial effect of inboard rotation upon the trimming action of the vertical tail surfaces, particularly for twin tail 4, which under NACA specifications ($\beta = 0°$) appears to be partly immersed in the slipstream jet. Reference 4 also concludes that outboard rotation causes the slipstream jet to diverge. Consequently, this mode of rotation increases the tail effectiveness at large angles of yaw but is less satisfactory in this respect than the inboard mode of rotation for other angles of yaw. This reasoning explains the favorable effect of outboard propeller rotation upon twin tail 4 when operating at an angle of sideslip of 10°. At this angle, owing to its original lateral displacement, this tail lies within the slipstream.

The data obtained in the tests indicate that for twin-engine airplanes equipped with single vertical tails and conventional right-hand propellers, the failure of a left engine will impose the more severe flight conditions. For airplanes equipped with twin vertical tails, however, the failure of a right engine should prove more critical to the fulfillment of the Army requirements. Similarly, it may be reasoned that use of propellers rotating inboard on both wings (symmetric rotation) would be advantageous for airplanes equipped with single fins both to improve tail effectiveness and to make the handling of controls similar regardless of the location of the

inoperative engine. Conversely, symmetric outboard rotation
should be favorable for airplanes equipped with twin fins.

Effect of Vertical-Tail Design

Effect of vertical-tail area.- The effect of varying
vertical-tail area was obtained from a study of the test
data for geometrically similar tails 1, 2, and 3. The
data for these tails with rudder fixed were converted to
values of full-scale brake horsepower and plotted in
figure 20.

The data of figure 20(a) show that increasing the
vertical-tail area resulted in increases in the asymmetric
power balanced by a given rudder deflection at zero angle
of sideslip. These increases, however, are not directly
proportional to the increase in tail (rudder) area, as
might normally be expected; this lack of proportionality
indicates the presence of secondary slipstream effects
upon the vertical tail surfaces. Such secondary effects
are probably produced by the sidewash angles generated
at the tail by inflow into the slipstream jet as well as
by the more direct effects of slipstream velocity.
Further investigation, however, is required to establish
a complete explanation of these secondary slipstream
effects.

The data in figure 20(b) illustrate the favorable
effect upon the asymmetric power characteristics of in-
creasing the vertical-tail area at an angle of sideslip
of 10°. These data show that, when the airplane is side-
slipping, the directional stability of the vertical tail
surfaces reinforces the action of the rudder control in
nullifying the effects of asymmetric power, and higher
values of asymmetric thrust can therefore be balanced
by a given vertical-tail arrangement. The magnitude
of the effects of directional stability can be obtained
from a study of the curve for a rudder deflection of
0° (fig. 20(b)), which is directly indicative of the
rudder-fixed directional stability. These data show
that the directional stability contributed by tail 1 barely
balanced the unstable yawing moments created by the yawed
fuselage-wing combination. Making the tail area larger
than that of tail 1 increased the directional stability,
as would be expected.

The effects of increasing tail area noted in the
tests with rudder fixed were also observed in the tests
with rudder free. Figure 11 illustrates the influence of
tail area upon the rudder-free trim characteristics of
the model operating under asymmetric power. In this
figure, the data indicate that freeing the rudder of
tail 1 was destabilizing, as would normally be expected
since the rudder type employed had a negative floating
ratio. Because of the slender margin of stability
associated with tail 1, the destabilizing action of
freeing the rudder was sufficient to cause directional
instability. Making the tail area greater than that of
tail 1 increased the directional stability contributed by
the tail surfaces sufficiently to overcome the destabiliz-
ing effects of the fuselage and, consequently, permitted
increases in the asymmetric thrust balanced by the vertical
tail surfaces.

Comparison of twin tail and single tail.- Twin tail 4
may be directly compared with tail 2 inasmuch as both
tails were of the same aspect ratio and equal area. Be-
cause the twin tail was located almost directly in the
slipstream, the twin tail was more effective than the
single tail at zero and small angles of sideslip. Figure 21
shows that the influence of power at $\beta = 0^\circ$ made
tail 4 almost as effective as tail 3, a surface of equal
aspect ratio but possessing 50 percent greater area. At
angles of sideslip greater than 0°, however, tail 4 was
less effective than tail 2 with the rudder fixed at an
angle of sideslip of 10° and with the rudder free (fig. 22).
These data confirm trends noted in the past and indicate
that the directional stability contributed by a twin
vertical tail is less than that contributed by a single
tail of the same aspect ratio and equal area. The in-
creased directional stability achieved by use of the
single tail is partly ascribed to the favorable end-plate
effect of the horizontal surfaces upon the load charac-
teristics of the vertical surfaces. In addition, the
single tail has but one root juncture compared with two
for the twin tail and therefore is less affected by inter-
ference effects.

It should be noted that the curves for tail 4 for
rudder free (fig. 22(b)) do not pass through the origin
but fall above and below it depending on the mode of
propeller rotation employed. These curves indicate that
reversing the propeller rotation altered the sidewash
caused by the propeller sufficiently to reverse the local
angle of attack of tail 4 at small angles of sideslip.

The results of the tests indicate that choice between single and twin vertical tails would depend largely upon the pilot's handling of the controls following a sudden engine failure. If the rudder control can be applied before the airplane reaches a moderately large angle of sideslip, the twin-tail design should be more suitable; otherwise, the single vertical-tail design would be preferable.

Effect of increasing aspect ratio.- The effect of increasing aspect ratio was determined from a comparison of the data obtained with tail 6, a surface of twice the aspect ratio of tail 2, with corresponding data for tails 2 and 3. These data are shown in figure 23 and indicate that doubling the aspect ratio of tail 2 has approximately the same effect as increasing the area by 50 percent at the same aspect ratio (tail 3). This effect is in close agreement with the wind-tunnel force data of reference 5, which show that doubling the aspect ratio of a surface from 1.5 to 3.0 increased the lift-curve slope from 2.2 to 3.1. For a given rudder configuration, such a change in lift-curve slope would result in an increase in total tail load, or trimming effectiveness, equivalent to that obtainable by approximately a 50-percent increase in area.

Comparison of conventional tail and all-movable tail with linked tab.- The question has been raised whether the efficient action of the all-movable tail reported in reference 6 arose largely from the "all-movable" feature or from the fact that the tail was of high aspect ratio and had the inherent advantages associated with tails of that type. For the present investigation, therefore, tests of the all-movable tail 5 were supplemented with tests of tail 7, which is identical with tail 5 except that tail 7 is of conventional - that is, fixed-fin - design.

A comparison of the effects of tails 5 and 7 upon the characteristics of the airplane operating with asymmetric power is shown in figure 24. These data indicate that the all-movable tail is markedly more effective than the conventional tail at zero sideslip with the rudder fixed and with the rudder free. At 10° sideslip and with rudder fixed, however, the all-movable tail was only slightly more effective than the conventional tail (fig. 24(a)).

These test results may be explained by use of the curves showing typical tail loads (fig. 25). These curves

show the variation of tail load with vertical-tail inci-
dence and rudder deflection for a conventional and an
all-movable tail. The tab area of the all-movable tail
is assumed equal to the rudder area of the conventional
tail. The variation of the load with deflection of the
all-movable tail is indicated by the dashed line in
figure 25. This variation is due to the linkage between
the tab and the movable forward surface. The slope of
the load curve is determined from the linkage ratio
δ_T/i_t which, for the case investigated, was equal to 1.12.
If the effect of power is ignored, the angle of attack
(tail incidence) of the conventional tail at $\beta = 0°$ is
also zero. The rudder deflection therefore produces
changes in load along a path coincidental with the zero
ordinate. For example, a rudder deflection of 10° produces
the tail load corresponding to the load indicated by
point a. For the all-movable tail, however, a rudder
deflection of 10° causes a simultaneous change in tail
angle of attack and tab deflection and produces the load
indicated by point b. Consequently, at zero sideslip,
the all-movable tail is capable of producing much larger
yawing moments with which to balance the effect of asym-
metric power than the conventional tail.

At moderate angles of sideslip (10° to 15°), the con-
ventional tail operates in the high-lift region of the
lift curve of the tail and consequently produces tail
loads of an order comparable with those produced by the
all-movable tail. The conventional tail may conceivably
produce tail loads even greater than those of the all-
movable tail because the conventional tail is unrestricted
in the use of rudder. The all-movable tail, however, is
limited for a given linkage ratio to the rudder deflection
that produces the tail incidence at maximum lift. Further
deflection would cause the entire surface to stall.

In balancing the effects of asymmetric power, the
superiority of the all-movable tail to the conventional
tail was most marked in the rudder-free tests. This su-
periority can be ascribed to the fact that the hinge-
moment characteristics of the all-movable tail force the
entire tail to float against the wind when free (positive
floating ratio) and consequently increase the directional
stability of the airplane. In considering the advantages
of the all-movable vertical tail over the conventional
tail, it should be observed that "snaking" oscillations
may be induced by control-surface friction with improperly
designed tails having positive floating ratios. (See
reference 6.)

Effect of rudder chord.- The effect of decreasing
rudder chord is shown by the test data for tails 6 and 7
(figs. 10 and 13). These data show that, although the
rudder of tail 7 had only one-half the area and one-half
the chord of the rudder of tail 6, the rudder of tail 7
balanced approximately two-thirds as much asymmetric power
at zero sideslip and approximately seven-eighths as much
power at 10° sideslip as the rudder of tail 6. These data
are in agreement with conventional trends because it is
known that decreasing the rudder chord increases the yaw-
ing moment per unit rudder area.

With rudder free, tail 7 balanced a greater amount
of asymmetric power than tail 6, which indicated a favorable
effect of reduced rudder area upon the rudder-free direction-
al stability. This action occurred because the rudders of
tails 6 and 7 are of the type that trail with the wind and
so reduce the directional stability when set free. Con-
sequently, tail 7, because of its smaller rudder area,
created smaller destabilizing moments when the rudder was
set free and so balanced a greater amount of asymmetric
power.

Effect of rudder deflection.- The data obtained in
the tests showed that increasing the rudder deflection
increased the amount of asymmetric power balanced by the
vertical tails at a decreasing rate.

Effect of dorsal and ventral fins.- The data illus-
trating the effect of adding dorsal- and ventral-fin areas
to tails 2, 3, 5, 6, and 7 are presented in figures 14 to
18. No data are presented for tail 1 because the addition
of dorsal and ventral fins did not noticeably lessen the
directional instability associated with this tail arrange-
ment.

The test data indicated that the addition of auxiliary
fin area increased the directional stability at large
angles of yaw and thereby increased the maximum amount of
asymmetric thrust balanced by the tail surfaces when the
rudders were free. Increases in maximum asymmetric thrust
of the order of 30 to 100 percent were observed in the
tests.

The addition of ventral-fin area was generally found
to be more effective than the addition of an equal amount
of dorsal-fin area. The use of a combination of dorsal-
and ventral-fin areas (dorsal a and ventral a) was

generally more effective than a single dorsal fin of the
same total area (dorsal b).

Aileron deflections required to trim asymmetric
thrust.- A representative plot of total aileron deflec-
tions required to trim the rolling moments created by
asymmetric thrust is presented in figure 26. These
deflections were always obtained by equal up-and-down
movements of the ailerons. Calculated values are also
presented in figure 26. These calculations were made
by using the method presented in reference 7. The calcu-
lated lift increments created by the operating propeller
were multiplied by the lateral arm of the propeller to
obtain rolling moments, which were converted to aileron
deflections required to trim by use of the data in figure 7.

The results presented in figure 26 show that, although
the scatter was considerable, the test data agreed fairly
well with the calculated values and indicated that moder-
ately large aileron deflections would be required to main-
tain straight flight under asymmetric power conditions.

CONCLUSIONS

The following conclusions were drawn from trim tests
of a twin-engine-airplane model operating under asymmetric
power (single-engine) conditions specified by the NACA and
Army Air Forces:

1. The direction of rotation of the operating pro-
peller had an important effect upon the asymmetric power
that could be balanced by a given vertical-tail design.
Single vertical tails were most effective when the oper-
ating propeller was rotating inboard. Twin tails, however,
were most effective when the operating propeller was
rotating outboard.

2. An all-movable vertical tail of aspect ratio 3
with a linked tab was more effective than the conventional
tail of the same aspect ratio and equal area in balancing
asymmetric power, particularly when the rudders were free.
The all-movable tail was markedly superior to the con-
ventional vertical tail of normal aspect ratio (1.5).

3. The single vertical-tail designs generally balanced
a greater amount of asymmetric power than twin vertical

tails of the same aspect ratio and equal area, particularly when the rudder was free. At small angles of sideslip, however, it was possible to balance more power by rudder deflection of the twin tails than by rudder deflection of a single tail.

4. Increasing the aspect ratio of a vertical tail resulted in increasing its trimming effectiveness under asymmetric power conditions by an amount proportional to the accompanying increase in lift-curve slope.

5. The trimming effectiveness of the vertical tail surface increased almost linearly with the vertical-tail area. Increasing rudder deflection and rudder chord increased the trimming effectiveness of the vertical tail under asymmetric conditions at a decreasing rate.

6. When the rudder was free, addition of dorsal- and ventral-fin areas increased the capacity of the vertical tail surfaces to balance asymmetric-power effects at moderate angles of sideslip.

Langley Memorial Aeronautical Laboratory
    National Advisory Committee for Aeronautics
        Langley Field, Va.

REFERENCES

1. Gilruth, R. R.: Requirements for Satisfactory Flying
      Qualities of Airplanes. NACA ACR, April 1941.
      (Classification changed to Restricted Oct. 1943.)

2. Anon.: Stability and Control Requirements for Air-
      planes. AAF Specification No. C-1815, Aug. 31, 1943.

3. Shortal, Joseph A., and Osterhout, Clayton J.:
      Preliminary Stability and Control Tests in the
      NACA Free-Flight Wind Tunnel and Correlation with
      Full-Scale Flight Tests. NACA TN No. 810, 1941.

4. Pitkin, Marvin: Free-Flight-Tunnel Investigation of
      the Effect of Mode of Propeller Rotation upon the
      Lateral-Stability Characteristics of a Twin-Engine
      Airplane Model with Single Vertical Tails of Dif-
      ferent Size. NACA ARR No. 3J18, 1943.

5. Zimmerman, C. H.: Characteristics of Clark Y Airfoils
      of Small Aspect Ratios. NACA Rep. No. 431, 1932.

6. Jones, Robert T., and Kleckner, Harold F.: Theory and
      Preliminary Flight Tests of an All-Movable Vertical
      Tail Surface. NACA ARR, Jan. 1943.

7. Pass, H. R.: Wind-Tunnel Study of the Effects of
      Propeller Operation and Flap Deflection on the
      Pitching Moments and Elevator Hinge Moments of a
      Single-Engine Pursuit-Type Airplane. NACA ARR,
      July 1942.

TABLE I.- INDEX TO FIGURES

Figure	Description	Remarks
1	Photographs of test model mounted on trim stand in Langley free-flight tunnel	Model with tail 2
2	Sketch of test model mounted on trim stand, which permitted freedom in yaw and roll, in Langley free-flight tunnel	
3	Three-view drawing of $\frac{1}{20}$-scale twin-engine model tested in Langley free-flight tunnel with asymmetric power	
4	Photograph of twin-engine model used in trim tests in Langley free-flight tunnel	Model with tail 2
5	Plan-form and dimensional characteristics of seven vertical tails tested on a $\frac{1}{20}$-scale model of a twin-engine airplane in the Langley free-flight tunnel	
6	Various fin arrangements tested with vertical tails on a $\frac{1}{20}$-scale model of a twin-engine airplane in the Langley free-flight tunnel	

Figure		Test specifications	Test condition	Tail arrangement			Operating-propeller rotation[1]	Curve	Remarks
				Tail	Dorsal	Ventral			
7		-----------	---------	2	------	-------	Propeller off	C_l against δ_a	Aileron calibration
8	a	NACA ($\beta = 0°$)	Rudder fixed	1 to 3	-------	-------	Inboard and outboard	T_c against δ_r	Directional-control run
	b	NACA ($\beta = 10°$)	Rudder fixed	1 to 3	-------	-------	------do------	T_c against δ_r	Do.
9	a	NACA ($\beta = 0°$)	Rudder fixed	4	------	-------	------do------	T_c against δ_r	Do.
	b	Army ($\beta = 10°$)	Rudder fixed	4	------	-------	------do------	T_c against δ_r	Do.
10	a	NACA ($\beta = 0°$)	Rudder fixed	5 to 7	------	-------	------do------	T_c against δ_r	Do.
	b	Army ($\beta = 10°$)	Rudder fixed	5 to 7	------	-------	------do------	T_c against δ_r	Do.
11	a	NACA (Rudder free)	Rudder free	1 to 3	------	-------	Outboard	T_c against β	Directional-stability run
	b	NACA (Rudder free)	Rudder free	1 to 3	------	-------	Inboard	T_c against β	Do.
12	a	NACA (Rudder free)	Rudder free	4	------	-------	Outboard	T_c against β	Do.
	b	NACA (Rudder free)	Rudder free	4	------	-------	Inboard	T_c against β	Do.
13	a	NACA (Rudder free)	Rudder free	5 to 7	------	-------	Outboard	T_c against β	Do.
	b	NACA (Rudder free)	Rudder free	5 to 7	------	-------	Inboard	T_c against β	Do.
14	a	NACA (Rudder free)	Rudder free	2	All combinations[2]		Outboard	T_c against β	Effect of dorsal- and ventral-fin area
	b	NACA (Rudder free)	Rudder free	2	------do------		Inboard	T_c against β	Do.
15	a	NACA (Rudder free)	Rudder free	3	------do------		Outboard	T_c against β	Do.
	b	NACA (Rudder free)	Rudder free	3	------do------		Inboard	T_c against β	Do.

[1]Right propeller operative.

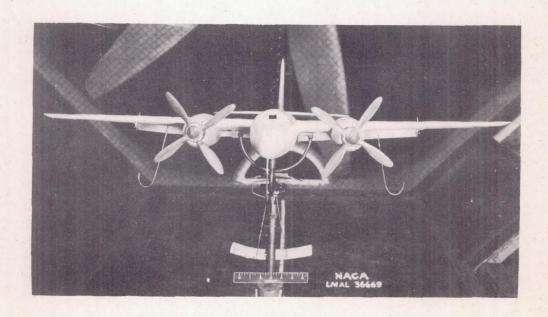[2]Combinations tested are tail alone, dorsal a, dorsal and ventral a, ventral a, dorsal b.

NATIONAL ADVISORY
COMMITTEE FOR AERONAUTICS

TABLE I.- INDEX TO FIGURES - Concluded

Figure		Test specifications	Test condition	Tail arrangement			Operating-propeller rotation[1]	Curve	Remarks
				Tail	Dorsal	Ventral			
16	a	NACA (Rudder free)	Rudder free	5	Tail alone, dorsal a, dorsal a and ventral a		Outboard	T_c against β	Effect of dorsal- and ventral-fin area
	b	NACA (Rudder free)	Rudder free	5	All combinations[2]		Inboard	T_c against β	Do.
17	a	NACA (Rudder free)	Rudder free	6	-----do-------		Outboard	T_c against β	Do.
	b	NACA (Rudder free)	Rudder free	6	-----do-------		Inboard	T_c against β	Do.
18	a	NACA (Rudder free)	Rudder free	7	-----do-------		Outboard	T_c against β	Do.
	b	NACA (Rudder free)	Rudder free	7	-----do-------		Inboard	T_c against β	Do.
19	a	NACA ($\beta = 0^\circ$)	Rudder fixed	1 to 7	------	--------	Inboard and outboard	bhp for $\delta_r = 20^\circ$	Effect of mode of rotation
	b	Army ($\beta = 10^\circ$)	Rudder fixed	1 to 7	------	--------	----------do----------	bhp for $\delta_r = 20^\circ$	Do.
	c	NACA (Rudder free)	Rudder free	1 to 7	------	--------	----------do----------	bhp for $10 < \beta < 12^\circ$	Asymmetric power balanced at verge of directional divergence
20	a	NACA ($\beta = 0^\circ$)	Rudder fixed	1 to 3	------	--------	Outboard	bhp against tail area	Curves of various rudder deflections
	b	Army ($\beta = 10^\circ$)	Rudder fixed	1 to 3	------	--------	---------do---------	-----do-----	Do.
21	a	NACA ($\beta = 0^\circ$)	Rudder fixed	2 to 4	------	--------	Inboard	bhp against δ_r	Comparison single and twin tail
	b	NACA ($\beta = 0^\circ$)	Rudder fixed	2 to 4	------	--------	Outboard	bhp against δ_r	Do.
22	a	Army ($\beta = 10^\circ$)	Rudder fixed	2, 4	------	--------	Inboard and outboard	bhp against δ_r	Do.
	b	NACA (Rudder free)	Rudder free	2, 4	------	--------	----------do----------	bhp against β	Do.
23	a	NACA ($\beta = 0^\circ$)	Rudder fixed	2, 3, 6	------	--------	Inboard	bhp against δ_r	Effect of aspect ratio
	b	NACA (Rudder free)	Rudder free	2, 3, 6	------	--------	----------do----------	bhp against β	Do.
24	a	NACA ($\beta = 0^\circ$) Army ($\beta = 10^\circ$)	Rudder fixed	5, 7	------	--------	Outboard	bhp against δ_r	Comparison of all-movable and conventional tail
	b	NACA (Rudder free)	Rudder free	5, 7	------	--------	----------do----------	bhp against β	Do.
25		-----------	-----------	----	------	--------	--------------------	Tail load against i_t	Illustrative of principle of all-movable tail
26		-----------	-----------	----	------	--------	Inboard and outboard	T_c against δ_a	Aileron deflections required to trim

[1]Right propeller operative.

[2]Combinations tested are tail alone, dorsal a, dorsal and ventral a, ventral a, dorsal b.

Figure 1.- Test model mounted on trim stand in Langley
free-flight tunnel.

WINDMILLING PROPELLER

COIL SPRING

BEARING A

PITCH BEARING LOCKED AT 5°
ANGLE OF ATTACK FOR ALL TESTS

OPERATING PROPELLER

BEARING B

TRIMMING FIN

ANGLE-OF-BANK INDICATOR

WIND

NATIONAL ADVISORY
COMMITTEE FOR AERONAUTICS
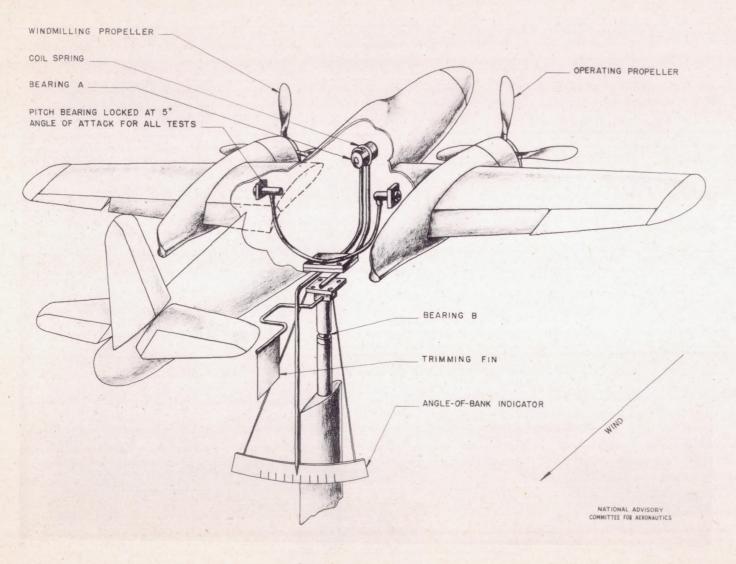
FIGURE 2.— TEST MODEL MOUNTED ON TRIM STAND IN LANGLEY FREE-FLIGHT TUNNEL. MODEL HAS FREEDOM IN
YAW AND ROLL.

Fig. 2
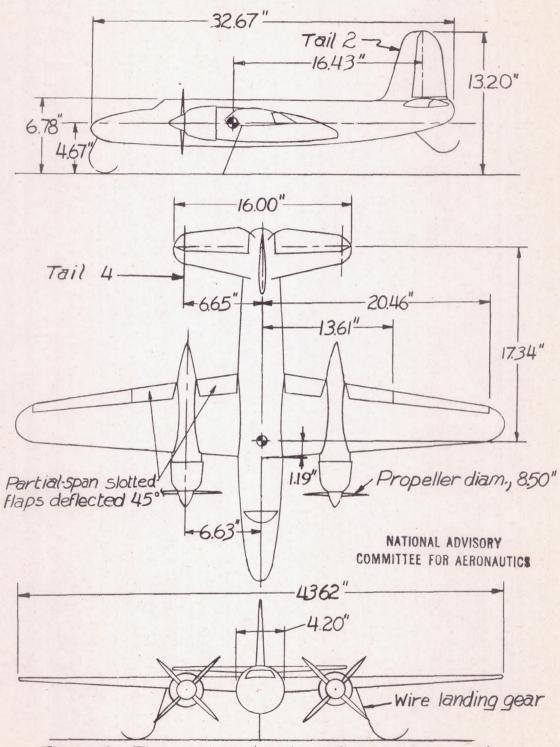
Figure 3.- Three-view drawing of 1/20-scale twin-engine model as tested in Langley free-flight tunnel with asymmetric power.

NACA LMAL 27625

NACA LMAL 27627
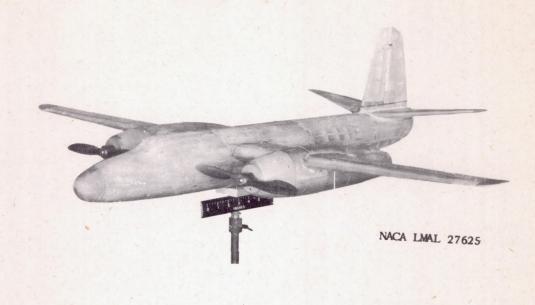
Figure 4. - Twin-engine model of B-28 airplane used in trim
tests in Langley free-flight tunnel.

	Tail						
	1	2	3	4	a5	6	7
Area, percent S_w	5.50	11.0	16.5	11.0	11.0	11.0	11.0
S_b, percent S_r	12.2	12.2	12.2	12.2	12.2	12.2	12.2
A	1.54	1.54	1.54	1.54	3.0	3.0	3.0
S_r, percent S_b	46.0	46.0	49.3	46.0	25.0	46.0	25.0

a Tail 5 pivots about 0.27 M.A.C.
HL of all tails 16.43" behind c.g.

NATIONAL ADVISORY
COMMITTEE FOR AERONAUTICS
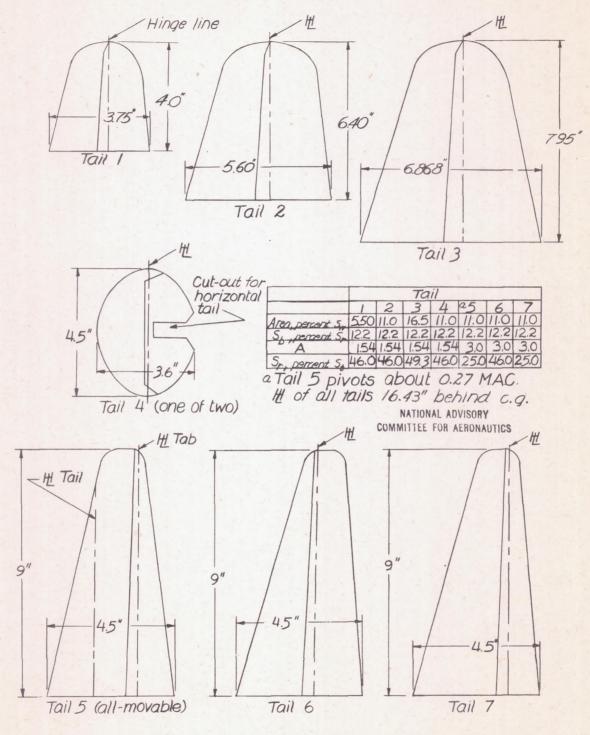
Figure 5.– Plan-form and dimensional characteristics of seven vertical tails tested on a 1/20-scale model of a twin-engine airplane in the Langley free-flight tunnel.

Fin	Area, percent S_t
Dorsal a	10
Dorsal b	20
Ventral a	10

Tail 2

Tail 3

Tails 5,6,7

Tail 1

NATIONAL ADVISORY
COMMITTEE FOR AERONAUTICS
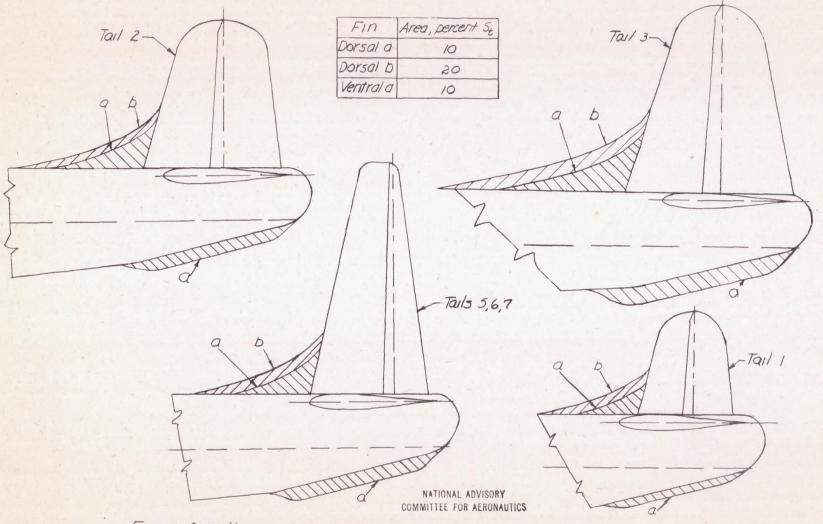
Figure 6.— Various fin arrangements tested with vertical tails on 1/20-scale model of a twin-engine airplane in the Langley free-flight tunnel.

Fig. 6
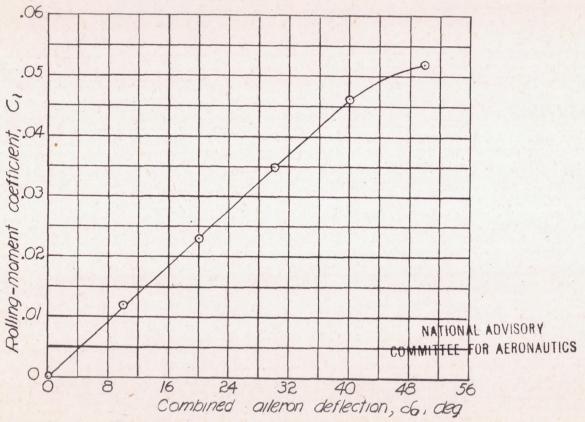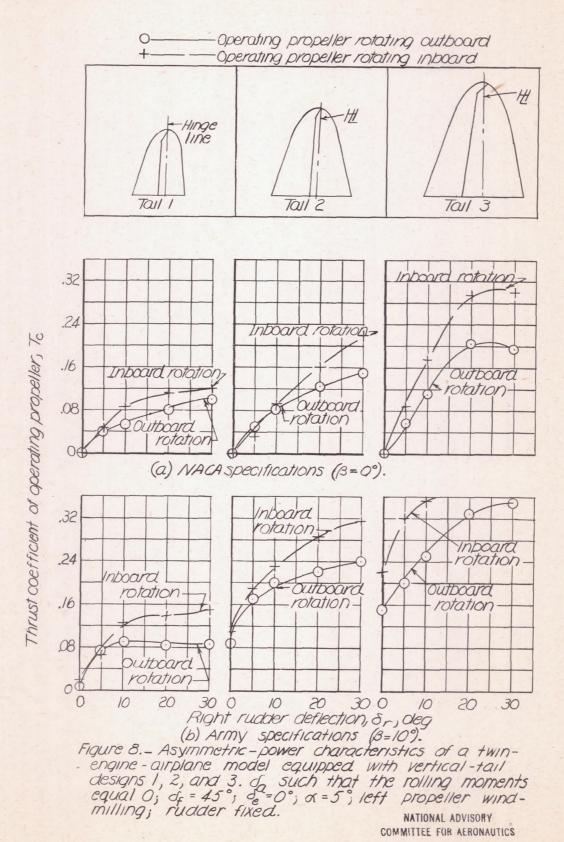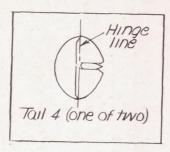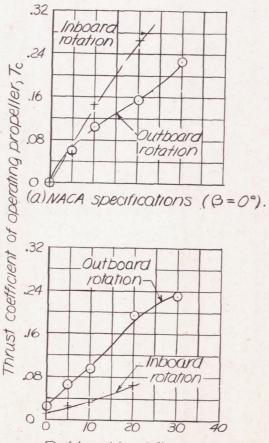
Figure 7. – Rolling-moment coefficients created by ailerons installed on test model in free-flight-tunnel investigation of asymmetric-power effects.

Fig. 7

Figure 8.— Asymmetric-power characteristics of a twin-engine-airplane model equipped with vertical-tail designs 1, 2, and 3. δ_a such that the rolling moments equal 0; $\delta_f = 45°$; $\delta_e = 0°$; $\alpha = 5°$; left propeller wind-milling; rudder fixed.

NATIONAL ADVISORY
COMMITTEE FOR AERONAUTICS

○————— Operating propeller rotating outboard
+————— Operating propeller rotating inboard

Figure 9.- Asymmetric-power characteristics of a twin-engine-airplane model equipped with vertical-tail design 4. δ_a such that the rolling moments equal 0, $\delta_f = 45°$; $\delta_e = 0°$; $\alpha = 5°$; left propeller windmilling; rudder fixed.
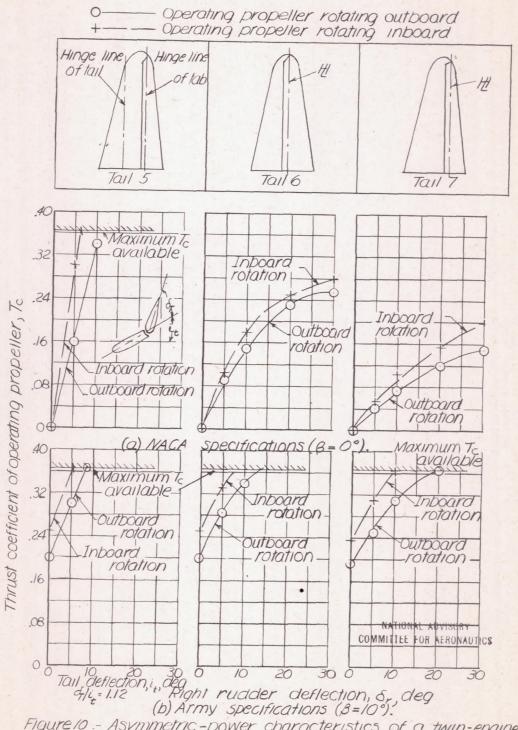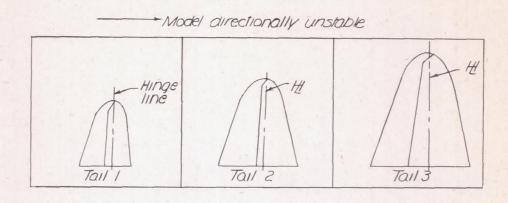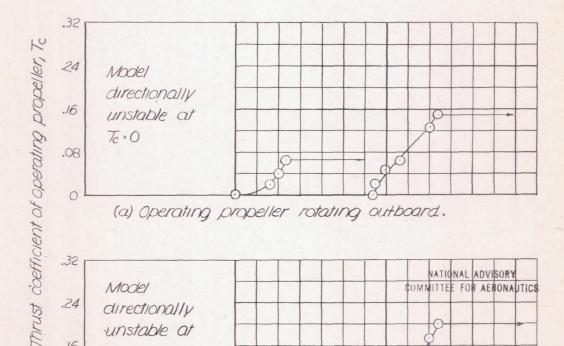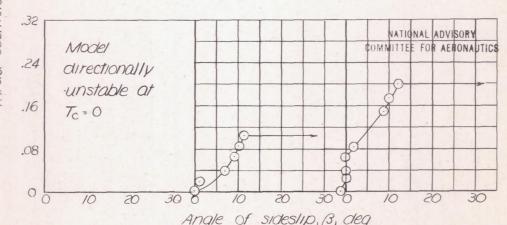
Figure 10.- Asymmetric-power characteristics of a twin-engine-airplane model equipped with vertical-tail designs 5, 6, and 7. δ_a such that the rolling moments equal 0; $\delta_f = 45°$; $\delta_e = 0°$; $\alpha = 5°$; left propeller windmilling; rudder fixed.

→ *Model directionally unstable*

Tail 1   Tail 2   Tail 3

(a) Operating propeller rotating outboard.

(b) Operating propeller rotating inboard.

Thrust coefficient of operating propeller, T_c

Angle of sideslip, β, deg

Figure 11.—Asymmetric-power characteristics of a twin-engine-airplane model equipped with vertical-tail designs 1, 2, and 3. δ_a such that the rolling moments equal 0; $\delta_f = 45°$; $\delta_e = 0°$; $\alpha = 5°$; left propeller windmilling; rudder free.

Model directionally unstable
○ ———— Vertical tail alone

Tail 4
(one of two)

.32

.24

.16

.08

0

(a) Operating propeller
rotating outboard.

.32

.24

.16

.08

0

NATIONAL ADVISORY
COMMITTEE FOR AERONAUTICS

-10   0   10   20   30
Angle of sideslip, β, deg

Thrust coefficient of operating propeller, T_c
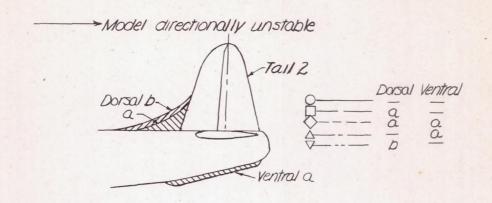
(b) Operating propeller rotating inboard.

Figure 12.- Asymmetric-power characteristics of a twin-engine-
airplane model equipped with vertical-tail design 4.
δ_a such that the rolling moments equal 0; δ_f = 45°; δ_e = 0°; α = 5°;
left propeller windmilling; rudder free.

Figure 13 .- Asymmetric-power characteristics of a twin-engine-airplane model equipped with vertical-tail designs 5, 6, and 7. δ_a such that the rolling moments equal 0; $\delta_f = 45°$; $\delta_e = 0°$; $\alpha = 5°$; left propeller windmilling; rudder free.
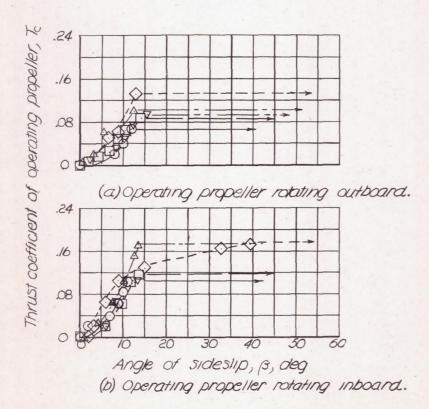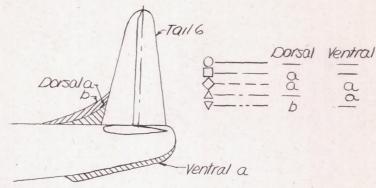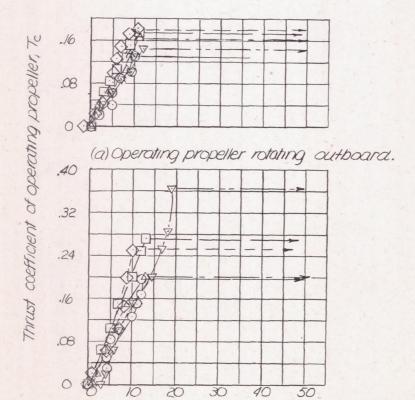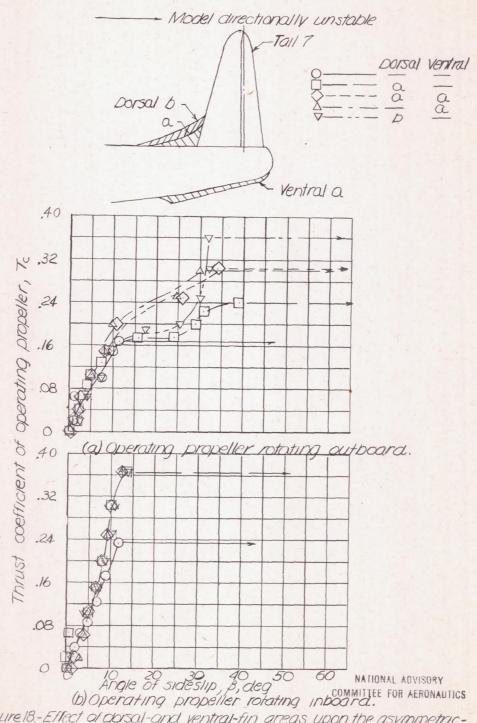
Figure 14.- Effect of dorsal-and ventral-fin areas upon
the asymmetric-power characteristics of a twin-engine-
airplane model equipped with vertical-tail design 2.
δ_a such that the rolling moments equal 0; $\delta_f = 45°$; $\delta_e = 0°$;
$\alpha = 5°$; left propeller windmilling; rudder free.

NATIONAL ADVISORY
COMMITTEE FOR AERONAUTICS

Model directionally unstable.

Tail 3

Dorsal b

a

Dorsal Ventral

Ventral a

Thrust coefficient of operating propeller, T_c

.32

.24

.16

.08

(a) Operating propeller rotating outboard.

.32

.24

.16

.08

0

0   10   20   30   40   50   60

Angle of sideslip, β, deg

(b) Operating propeller rotating inboard.
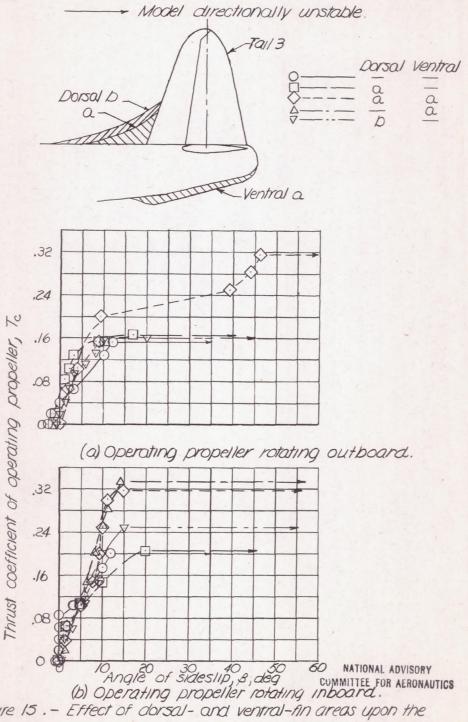
Figure 15.— Effect of dorsal- and ventral-fin areas upon the asymmetric-power characteristics of a twin-engine-airplane model equipped with vertical-tail design 3. δ_a such that the rolling moments equal 0; $\delta_f = 45°$; $\delta_e = 0°$; $\alpha = 5°$; left propeller windmilling; rudder free.
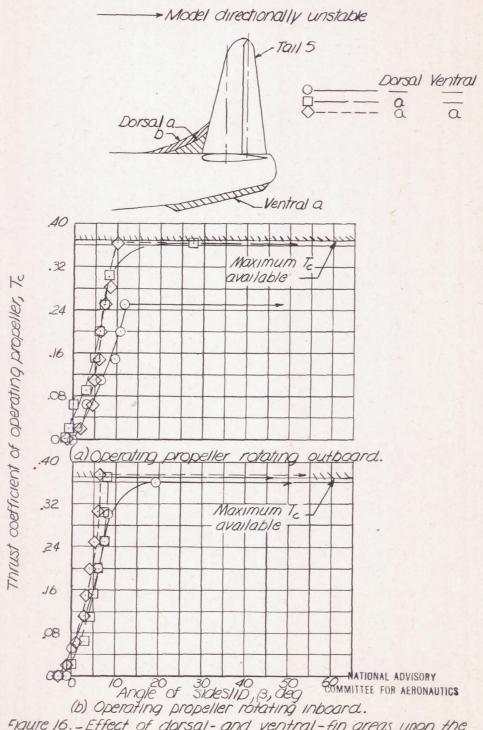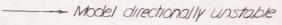
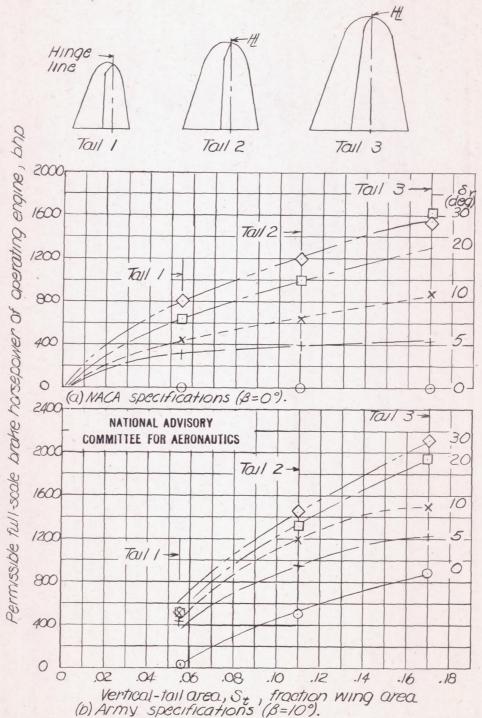Figure 16.- Effect of dorsal- and ventral-fin areas upon the asymmetric-power characteristics of a twin-engine-airplane model equipped with vertical-tail design 5. δ_a such that the rolling moments equal 0; $\delta_f = 45°$; $\delta_e = 0°$; $\alpha = 5°$; left propeller windmilling; rudder free.

Figure 17.- Effect of dorsal-and ventral-fin areas upon the asymmetric-power characteristics of a twin-engine-airplane model equipped with vertical-tail design 6. δ_a such that the rolling moments equal 0; $\delta_f = 45°$; $\delta_e = 0°$; $\alpha = 5°$; left propeller windmilling; rudder free.
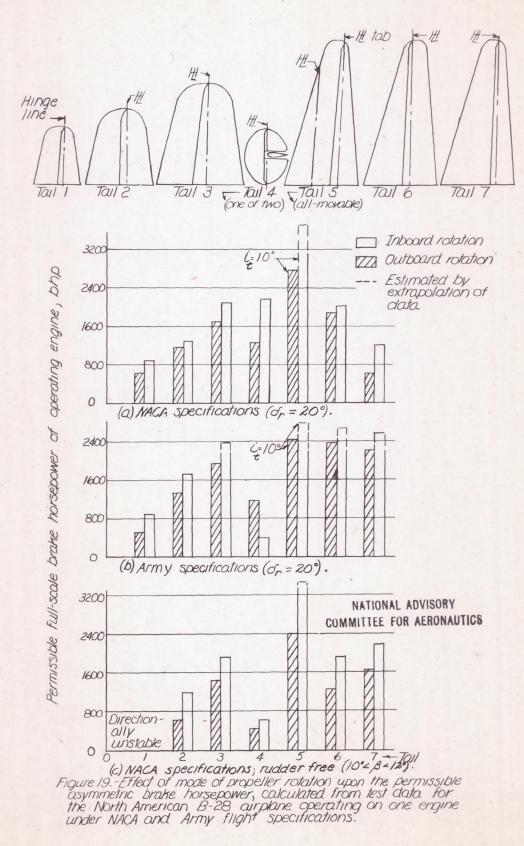
Figure 18.- Effect of dorsal- and ventral-fin areas upon the asymmetric-power characteristics of a twin-engine-airplane model equipped with vertical-tail design 7. δ_a such that the rolling moments equal 0; $\delta_f = 45°$; $\delta_e = 0°$; $\alpha = 5°$; left propeller windmilling; rudder free.

Figure 19.- Effect of mode of propeller rotation upon the permissible asymmetric brake horsepower, calculated from test data for the North American B-28 airplane operating on one engine under NACA and Army flight specifications.

Figure 20.- Effect of vertical-tail area and rudder deflection upon the permissible brake horsepower, calculated from model test data, for the North American B-28 airplane operating on one engine under NACA and Army flight specifications. Operating propeller rotating outboard.
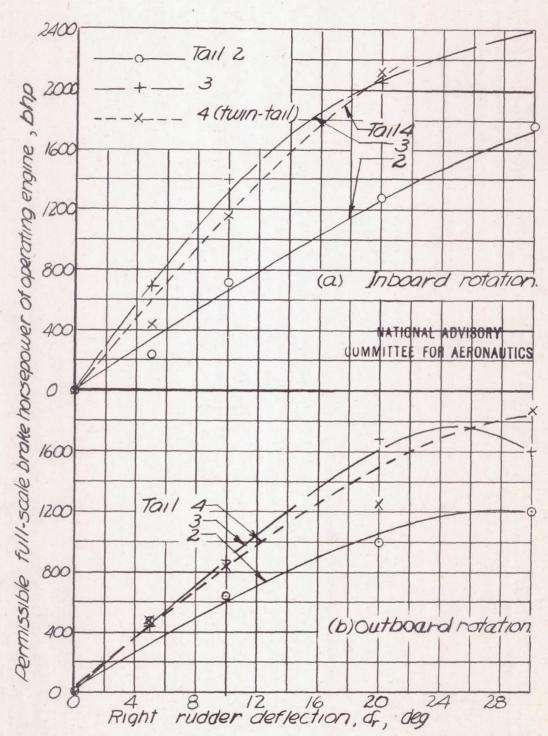
Figure 21.- Comparison of the asymmetric-power characteris-
tics of an airplane equipped with twin and single
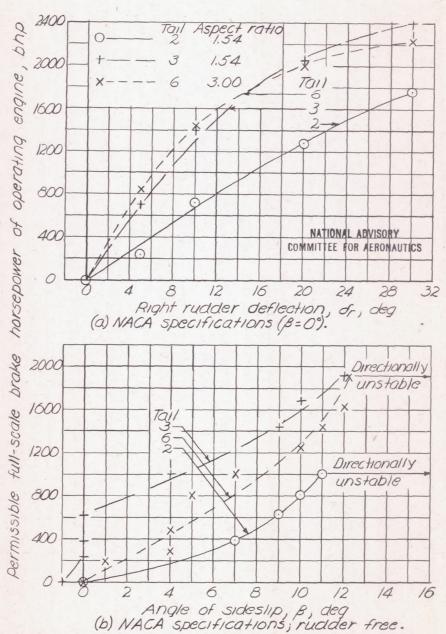vertical tails. NACA specifications; $\beta = 0°$.

(a) Army specifications (β=10°).

(b) NACA specifications; rudder free.
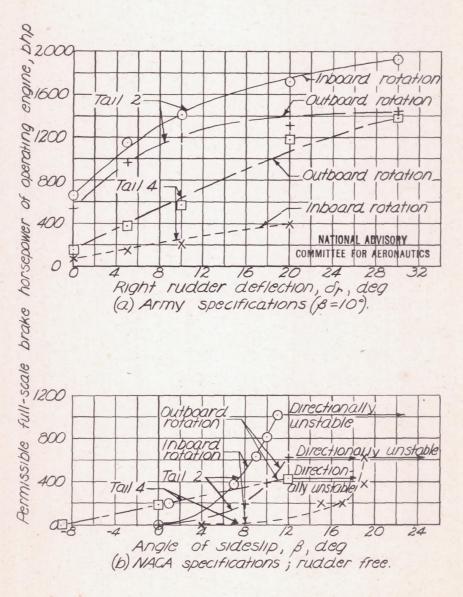
Figure 22.- Comparison of the asymmetric-power characteristics of an airplane equipped with twin and single vertical tails and at various angles of sideslip.

(a) NACA specifications ($\beta = 0°$).

(b) NACA specifications; rudder free.

Figure 23.– Comparison of the asymmetric–power characteristics of an airplane equipped with high- and low-aspect-ratio vertical tails. Inboard rotation.
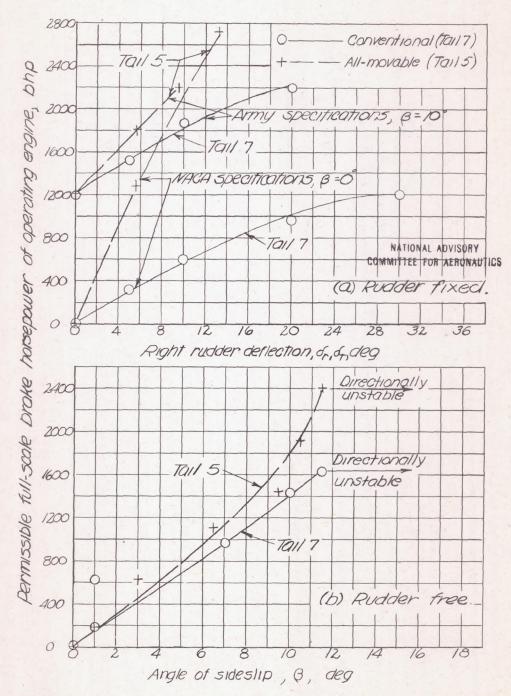
Figure 24.- Comparison of the asymmetric-power charac-
teristics of a twin-engine-airplane model equipped
with an all-movable vertical tail with linked tab
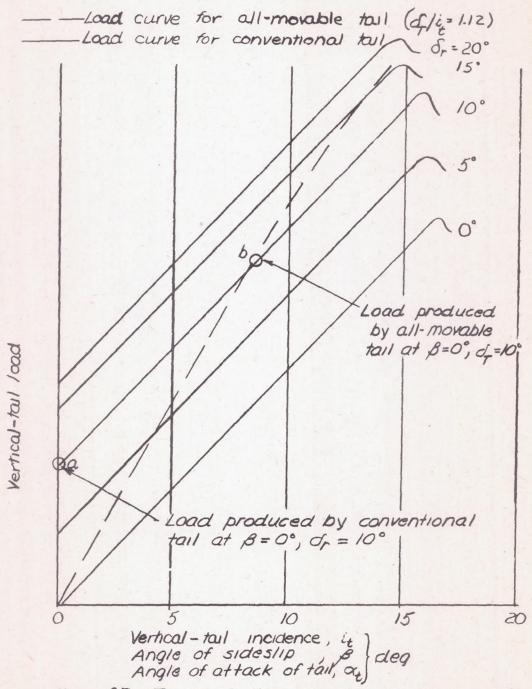and with a single conventional tail. Operating
propeller turning outboard.

——— Load curve for all-movable tail ($d_f/i_t = 1.12$)
——— Load curve for conventional tail

Figure 25.- Typical load curves for the all-movable and conventional types of vertical tail.
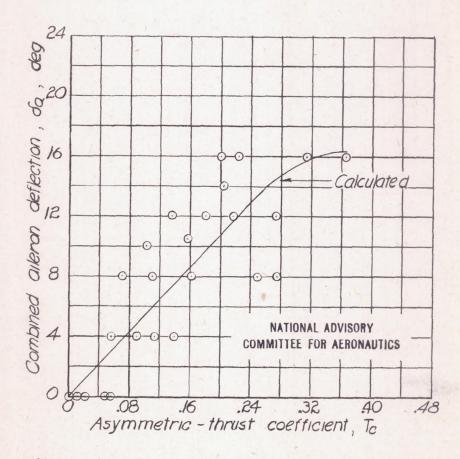
Figure 26.— Aileron deflections required to trim
         rolling moment created by asymmetric
         power. β = 0°; operating propeller
         rotating outboard.